water

MDPI

Article

Identification of Hydrochemical Characteristics, Spatial Evolution, and Driving Forces of River Water in Jinjiang Watershed, China

Yuchen Zhu [1,2], Hongjie Yang [3], Yong Xiao [3,*], Qichen Hao [1,2], Yasong Li [1,2], Jiahuan Liu [1,2], Liwei Wang [3], Yuqing Zhang [3], Wenxu Hu [3] and Jie Wang [3]

1 Fujian Provincial Key Laboratory of Water Cycling and Eco-Geological Processes, Xiamen 361021, China; zhuyuchen413@163.com (Y.Z.); haoqichen_iheg@163.com (Q.H.); liyasong712@126.com (Y.L.); liujiahuan1105@163.com (J.L.)

2 Institute of Hydrogeology and Environmental Geology, Chinese Academy of Geological Science, Shijiazhuang 050061, China

3 Faculty of Geosciences and Environmental Engineering, Southwest Jiaotong University, Chengdu 611756, China; yanghj@my.swjtu.edu.cn (H.Y.); leeway@my.swjtu.edu.cn (L.W.); zhangyuq@my.swjtu.edu.cn (Y.Z.); hwxxwh@my.swjtu.edu.cn (W.H.); cfqswangjie@my.swjtu.edu.cn (J.W.)

* Correspondence: xiaoyong@swjtu.edu.cn

Abstract: Rivers are an important source of water in humid regions, but their availability is greatly limited by water chemistry. In order to accurately identify the changes in river water chemical composition, the compositional analysis method (CoDA) is proposed from the perspective of compositional data analysis theory, which considers the geochemical riverine system as a whole and detects the compositional changes of the entire watershed. The basic data analysis is carried out by traditional analysis methods, and the results show that the hydrochemical characteristics of different sections of the basin have significant features. The water chemistry of Dongxi River is of the HCO_3^- Ca type. The water of the Xixi River shows a gradual evolution from the HCO_3-Ca type and high SO_4^{2-} content in the upper reaches to the Cl-Ca type in the lower reaches. The hydrochemistry of river water in the watershed is mainly affected by rock weathering leaching (PC1) and agricultural and domestic pollutant discharge (PC2), with a contribution rate of 48.4% and 19.7%, respectively. Rock weathering, mining, and agricultural pollution are the main factors affecting the chemical composition of river water in different regions. The spatial composition of a single sample at different scales is monitored by the Mahalanobis distance approach in an iterative manner to minimize the influence of a single anomaly on the composition center. The results show that the main reasons for the change in river water chemical composition along the Xixi River are attributed to mine pollution, domestic pollution, and tea plantation and that along the Dongxi River is caused by domestic pollution. The hydrochemical composition changes after the confluence of the Xixi River and Dongxi River are mainly affected by human activities and seawater in urban areas. This research could provide new perspectives and methods for detecting the influences of human and natural factors on the hydrochemistry of river water in humid regions worldwide.

Keywords: hydrochemistry; human activity; component data analysis; Mahalanobis distance; Jinjiang watershed

check for updates

Citation: Zhu, Y.; Yang, H.; Xiao, Y.; Hao, Q.; Li, Y.; Liu, J.; Wang, L.; Zhang, Y.; Hu, W.; Wang, J. Identification of Hydrochemical Characteristics, Spatial Evolution, and Driving Forces of River Water in Jinjiang Watershed, China. *Water* **2024**, *16*, 45. https://doi.org/10.3390/w16010045

Academic Editor: Elias Dimitriou

Received: 16 November 2023
Revised: 16 December 2023
Accepted: 18 December 2023
Published: 21 December 2023

1. Introduction

The water resource is the most important natural and strategic resource, which plays a key role in maintaining the stability of the natural ecosystem and developing the economy of human society [1]. As one of the main components of freshwater resources, surface water is favored because it is easy to obtain and utilize. However, surface water is also the most vulnerable to be influenced by external factors [2–4]. With the rapid development of the economy, the quality and quantity of surface water were greatly affected because water resource was in huge demand, and domestic sewage and industrial effluent were discharged into the surface water without meeting the discharge requirements [1,5,6]. Hence, it is of immense significance to study the surface water of the basin in depth for better protection and utilization of surface water resources, and it is also beneficial to alleviate the contradiction of water resource shortage [7–9].

Surface water formation is the result of the interaction between the development of rivers and the environment, and it will be affected by groundwater recharge, rock weathering, atmospheric precipitation, human activities, and other effects [4,10]. In most cases around the world, groundwater is one of the main recharge sources for surface water. In mountainous areas, groundwater feeds into surface water in the form of springs or underground rivers, and the mixing of surface water and groundwater will affect the hydrogeochemical composition of surface water [11–13]. Along with the runoff process, the river will exchange materials with the surrounding land, and different types of land use will also affect the materials exchanged with the surface water [14,15]. In recent years, the global temperature change caused by drastic climate change has also directly affected the precipitation recharge and evaporation of surface water [4,16–18]. In addition, in coastal areas, seawater backflow can also alter river hydrochemistry [19].

In addition to natural factors, human activity is also an important part, which affects the physical and hydrochemical properties of surface water [20]. Around the world, rivers are disturbed by human activities to varying degrees [21]. For example, the development of mines may introduce some unique elements into the river [22]. The discharge of untreated sewage can cause the water quality of rivers to decline [23]. Fertilizers applied in agriculture can also find their way into rivers [24]. Human activities have changed the composition of rivers and posed a great threat to surface water resources. Because the physical and hydrochemical properties of the surface water in the basin are the comprehensive embodiment of the hydrological environment conditions and human activities, it contains abundant hydrogeological information.

The analysis of hydrogeochemical characteristics is the basis of studying hydrochemical composition and water quality evolution [25,26]. In order to interpret the abundant information in surface water, scholars have been exploring the hydrochemical characteristics of rivers. On the basis of a large number of practical cases, Gibbs summarized three mechanisms controlling surface hydrochemistry, atmospheric precipitation, rock weathering, and evaporation, respectively, which have been widely used by later generations. The Piper diagram is used to determine the type of hydrochemistry, etc. Some multivariate statistical methods such as hierarchical cluster analysis (HCA) and principal component analysis (PCA) are also used in the analysis of the hydrochemistry [27,28]. However, these river hydrochemistry analyses mainly focus on the statistics and spatial distribution of the main components in the water body, which cannot be comprehensively analyzed as a whole. And they are easy to be affected by component anomalies that are caused by some accidental factors during sampling, thus obtaining some unreliable or wrong conclusions.

In order to eliminate these effects, component data analysis (CoDA) is used to solve the problem. The component data analysis method considers the properties of the component data, combined with the Mahalanobis distance [29]. It considers each hydrochemical component as a whole and obtains the overall characteristics of the multi-component system [30]. Based on component data analysis, the variation characteristics of basin hydrochemistry can be comprehensively evaluated, and the interference of individual regional anomalies can be identified, which has guiding significance for monitoring potential pollution events and local climate-induced changes at the basin scale.

The Jinjiang river, located in the southwest of China's Fujian Province, serves as a major source for local water demand. With the rapid development of urbanization and economy in southwest Fujian, the hydrochemical components of Jinjiang watershed have changed significantly under the combined influence of climate change and human-made pollution [31]. In recent years, scholars have mainly conducted in-depth studies on typical pollutants in the water bodies of Jinjiang watershed, such as nitrogen and phosphorus, organics, and heavy metals. However, the existing hydrochemical analysis is mostly focused on the small watersheds in the downstream urban area, and the hydrochemical components covering the whole Jinjiang watershed have not been comprehensively and systematically analyzed.

This paper in view of the river water hydrochemical characteristics of the Jinjiang watershed, which are strongly influenced by human activities, based on the CoDA method, systematically collected and tested the water samples of the upper and lower reaches and tributaries of Jinjiang watershed. The specific aims are to (1) consider the obtained hydrochemical component data as a whole and analyze the hydrochemical components of the whole basin by using biplot and Mahalanobis distance calculations, based on the CoDA method; (2) identify the composition change and variation rules of hydrochemical components in Jinjiang watershed; (3) explain the influence and contribution of natural conditions and human factors on river hydrochemical components; and (4) provide suggestions for the utilization and protection of water resources in Jinjiang watershed.

2. Study Area

Jinjiang is located in the southeast part of the Fujian province, southeastern China. The Jinjiang watershed is defined within the latitude range of 24°45′ N to 25°35′ N and the longitude range of 117°40′ E to 118°42′ E, with an approximate total area of 5606 km^2. It flows from northeast to southeast with a total length of 404.8 km and runs through Yong Chun County, Anxi County, Nan'an City, Licheng District, and Jinjiang City. This watershed is covered by mountains and hills for 81.4% of the whole area. The plain topography only accounts for approximately 18.6% of the watershed and is distributed in the coastal area in the southeast, which has the largest city—Jinjiang, the most densely populated area in the watershed. This watershed is featured by the typical summer monsoon climate with an average annual rainfall of 1686 mm. But the rainfall presents significant uneven characteristics temporally, with 71.2% occurring from April to September [32].

The Jinjiang watershed includes two major tributaries, namely, Dongxi (West Creek) and Xixi (East Creek). In more detail, it can be divided into five sections, based on the water catchments of the tributaries, which are Xixi tributaries, Xixi mainstream, Dongxi tributaries, Dongxi main stem, and the lower course of Jinjiang, respectively (Figure 1). Dongxi (West Creek) and Xixi (East Creek) are located in the middle-upper area of the watershed. These two tributaries cover an area of 1917 km^2 and 3101 km^2, respectively. Dongxi and Xixi originate from the snowy mountains of Chengxiang in Yongchun and Tiziling, Taozhou in Anxi. Dongxi and Xixi converge at Shuangxi in Nan'an City and finally merge into Quanzhou Bay at Qianpu. The Shanmei Reservoir built in Dongxi is the only water conservancy hub in Jinjiang watershed [33]. The average discharge of the main branch is 5.12 billion m^3 per year, which peaks in the mountainous areas in the upper course and then falls gradually as it flows downstream through lower coastal plains [34]. In contrast, the population distribution and economic development are gradually stronger as the river flows downstream [35].

The strata exposed in Jinjiang watershed are mainly Triassic, Jurassic, and Quaternary, among which the volcanic rocks of the Upper Jurassic Nangyuan Formation are the most widely distributed, and the lithology is mainly tuff. Among the igneous rocks, late Jurassic volcanic rocks and Yanshan-age intrusive rocks are widely exposed. The chemical composition of the exposed strata shows homogeneity [35,36], all of which are dominated by silicate rocks, but the strata contain a variety of metallic and non-metallic ores, such as kaolinite, molybdenum, tungsten, iron, manganese, copper, and zinc, making a wide range of types of mines within Jinjiang watershed. With the rapid development of regional industry and agriculture in recent years, a large number of pollutants (nitrogen and phosphorus nutrient use, iron and manganese mining, etc.) have entered the river, making the quality of the water environment in the basin gradually deteriorate [37–39].

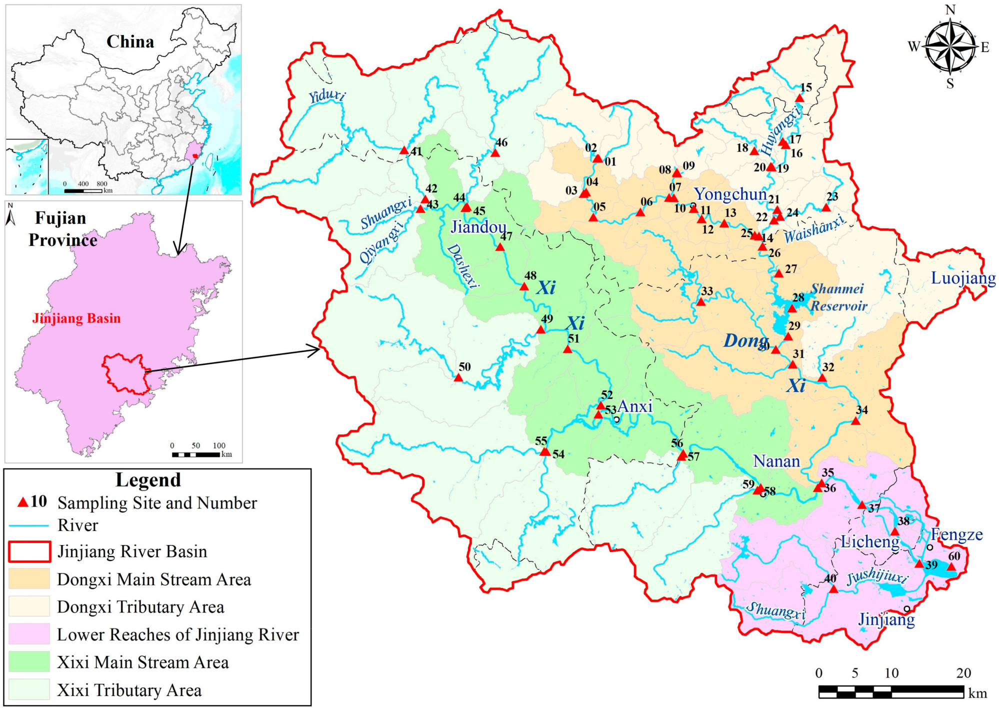

Figure 1. Location of the study area and the river water sampling sites.

Groundwater in Jinjiang watershed is mainly distributed in aquifers of unconsolidated rock pores, weathered eluvial pores and fractures, and bedrock fissures. The porous water in loose rock formations is mainly distributed in the terraces on both sides of the valley, the alluvial fans in front of the mountains, and the marine sedimentary formations in the coastal estuary areas, mainly composed of fine sand, coarse sand, and gravel, with a thickness of about 5–20 m and a specific yield of less than 100 $m^3/d \cdot m$. In some areas near the river, the groundwater receives water supply from the river, and the specific yield can exceed 100 $m^3/d \cdot m$ [40]. Weathered fissures are mainly distributed at the foot of tablelands and piedmont slopes, with the aquifer composed of clastic rock and conglomerate generally having a thickness of 10–20 m and a relatively low water volume, with a specific yield of 10 $m^3/d \cdot m$. Bedrock fissure water is distributed in the fractures and faults of mountainous bedrocks, with the water yield controlled by structural faults. Its water content is extremely uneven, with an overall low water volume and a specific yield of about 10 $m^3/d \cdot m$. Groundwater recharge mainly comes from the vertical infiltration of atmospheric precipitation and the lateral infiltration of rivers during the rainy season.

3. Data and Methods

3.1. Sample Collecting and Analytic Testing

Based on data from the Shuttle Radar Topography Mission (SRTM), the basin is divided into 60 drainage areas by using the ArcGIS hydrologic toolset, and at every confluence, we set a sampling spot, which adds up to cover the whole basin.

Water samples were collected from 5 to 20 June 2020 (rainy season). The sampling sites were distributed throughout Jinjiang watershed along the Jinjiang river and its tributaries (Figure 1). The water samples were collected the sample water from 150 cm deep in the middle of the stream to get rid of floating suspended pollutants as much as possible.

Water samples were collected in 2.5 L clean high-density polyethylene bottles that had been thoroughly prerinsed with the water to be sampled. The bottles used for trace element determination were acidified with nitric acid to pH < 2. All samples were stored in potable incubators at the temperature of 4 °C and transported to the Laboratory of Groundwater Sciences and Engineering of the Institute of Hydrogeology and Environmental Geology, Chinese Academy of Geological Sciences for hydrochemical analysis.

Water quality parameters such as total dissolved solids (TDS) and pH were measured and recorded on-site using a MANTA+30 multiparameter instrument (EUREKA, Austin, TX, USA). Major cations (Ca^{2+}, Mg^{2+}, Na^+, K^+) as well as some trace elements and ions (Fe, Mn, Zn, Pb) were determined using a full-spectrum plasma generation spectrometer (ICAP-6300, Tokyo, Japan) with a detection limit of 1 μg/L. ${SO_4}^{2-}$, Cl^- were measured using ion chromatography (Shimadzu LC-10ADvp, Tokyo, Japan). ${HCO_3}^-$ was measured by titration with hydrochloric acid [28]. Total phosphorus and total nitrogen were determined using potassium persulfate oxidation and UV spectrophotometer (UV 2450, Shimadzu, Kyoto, Japan) [41,42]. The consistency and accuracy of the analyzed results had been checked for quality assurance. Triplicate analyses were conducted for each sample to ensure the consistency of analyzed parameters. The accuracy of hydrochemical analysis for each sample was checked using the ionic charge balance error percentage (%CBE), which can be determined by Formula (1). The results showed that the recovery ratio was within ±10%, and the %CBE values were less than ±5% for all samples, implying that the analytical accuracy was reasonably good [43].

$$\%\text{CBE} = \left(\sum\nolimits_{\text{i}}^{\text{m}} \text{ce}_i^+ - \sum\nolimits_{\text{i}}^{\text{m}} \text{ce}_i^-\right) / \left(\sum\nolimits_{\text{j}}^{\text{m}} \text{ce}_j^+ - \sum\nolimits_{\text{j}}^{\text{m}} \text{ce}_j^-\right) \tag{1}$$

where ce_i^+ and ce_i^- are the charge concentration of a specific cation and anion, respectively, in milliequivalents per lit.

3.2. Component Data Analysis Methods

3.2.1. Log-Ratio Transformation and Biplot

The compositional data are influenced by constant row sum, leading to a "closure effect", causing null-correlation contained in the correlation structure of the data [44]. The multivariate statistical methods cannot be applied to the compositional data [45], and we have to transform the compositional data into a real number space [46]. Currently, the centered log-ratio transformation (CLR) [5] and isometric log-ratio transformation (ILR) [47] are commonly used. The formulas of CLR and ILR are as follows:

$$\text{CLR}(x) = \left(\ln \frac{x_i}{\text{g}(x)}\right) \tag{2}$$

$$\text{ILR}_i(x) = \sqrt{\frac{D-i}{D-i+1}} \ln \frac{\sqrt[D-i]{\prod_{j=i+1}^{D} x_j}}{x_i} \tag{3}$$

As shown in the formula, i represents the number of sample sites, $\text{g}(x)$ represents the geometric mean of the concentration of elements at each sample site, i.e., $\text{g}(x) = \sqrt[D]{x_1 \cdot x_2 \cdots x_D}$; among which, x_i represents the concentration of elements. D refers to dimensions, here it represents the number of variables.

We carried out robust principal component analysis (RPCA) on the transformed data to obtain the loadings and scores. Then we displayed them on the biplot in the form of a 2d multi-dimensional scatterplot [48,49]. The point coordination displays the scores of the principal components for two samples, and the distances between points approximate the correlation of two samples, meaning that the closer they are, the stronger the correlation. The vector length is proportional to the total variance of the variables, representing the component loading [50]. The projection length of the vector on the corresponding axis is the amount of variance described by each component variable captured by the corresponding principal component, i.e., characterizing the contribution of that component to the corresponding principal component of the axis, as shown in Figure 2. The vector length approximates the standard deviation of a column index. The $\cos(\alpha)$ represents the correlation between indexes. The projection of the sample point to the vector represents the value of the index at that point. Sample point spacing indicates the correlation between samples.

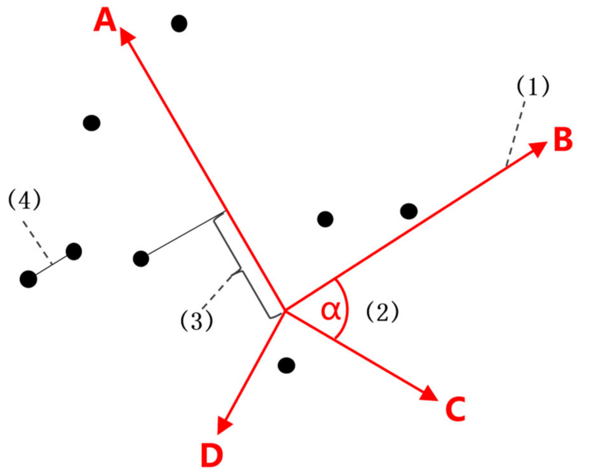

Figure 2. Description of the biplot. The point approximation represents the sample information (row information) of the transformed data matrix and the vectors approximation represent the metric information (column information) of the transformed data matrix. (1) The length of the vector approximates the standard deviation of a column of indicators. (2) The cos(α) represents the correlation between indexes. (3) The projection of a sample point onto a vector represents the value of the indices in that point. (4) The distances between points approximate the correlation of two samples.

3.2.2. Mahalanobis Distance

The Mahalanobis distance (MD) is a measure of the distance between points and centroid, which considers the multivariate covariance [51]. MD is usually used to identify outliers for multivariate data [52,53], and sometimes, it can also be used for the determination of representativity of data extracted from a larger population of samples [54]. When there are changes in the chemical composition of water in the river which are caused by inflows of tributaries with large differences in components and pollutants, it will be reflected as an increase in MD. The formula of MD is as follows:

$$D^2 = (x_i - \overline{x})S^{-1}(x_i - \overline{x})' \quad (4)$$

where, D^2 is MD, x_i is one of the indicators of the samples, which in this paper represents the element concentration; $\overline{x}$ is the average of the indicator, which represents the average value of the ion in the water's chemical composition; S^{-1} is the inverse matrix of the covariance matrix. By using log-ratio transformation, the data will be transformed from simplex space into real number space before MD can be calculated. This paper aims to show the anomaly between samples through the MD of the sample composition.

This paper uses R-package robCompositions to carry out CLR and ILR and uses the R-package FactoMineR, Factoextra to analyze the composition and draw the biplot [55]. The indicators with a detection rate lower than 40% were not involved in the analysis. Finally, the 12 indicators were chosen for analysis: $Na^+ + K^+$, Ca^{2+}, Mg^{2+}, $SO_4{}^{2-}$, $HCO_3{}^-$, Cl^-, Fe, Mn, Zn, Pb, TN, and TP; among which, those below the limit of detection (LoD) were replaced by 2/3 of the LoD. Based on the current land use type and the test results, 13 samples with little interference from human activities are selected (i.e., the samples that have the closest composition to their natural state, sample numbers: 02, 15, 16, 17, 18, 19, 20, 21, 22, 23, 24, 41, and 46) as the "original composition" and then calculate their composition center and the covariance matrix. MD is then calculated using the 60 water samples and the center of "original composition" and the analysis continues to examine the composition variations of the samples with the "original composition". After this, starting from the "original composition", every sample site of the main stem is added from upstream to downstream iteratively. The chemical composition centers of Xixi mainstream and Dongxi mainstream and the MD between every sample and the two composition centers are calculated. Finally, two clustered line charts with MD data of Xixi mainstream and Dongxi mainstream are drawn. The clustered line charts that use the results of iterative calculation of MD can minimize the influence of individual outliers on the whole trend. Except the advantage of visualizing the overall trends, the clustered line charts can also help identify the anomalies in the water's chemical composition.

4. Results and Discussion

4.1. Physicochemical Characteristics of River Water

Due to the significant differences in the natural environment and production and living conditions between the two main tributaries of Dongxi and Xixi, as well as the three downstream areas of Jinjiang, the differences in the characteristics of their respective tributaries and main streams are not significant. Therefore, in order to highlight the overall physical and chemical characteristics of the three areas, the sample data from the tributaries and main streams of Dongxi and Xixi will be combined and analyzed here.

The ranges of chemical compositions of cross-sectional water in Jinjiang watershed are statistically given in Table 1 and Figure 3. (It should be noted that the sample at Point 60, which are affected by seawater, show significant numerical differences from the other points and is not included in the statistical analysis in Table 1). The pH of river water ranges from 7.45 to 9.58, with an average value of 7.87, showing a weak alkalinity. The pH values of the Dongxi watershed are relatively higher than Xixi watershed and lower reaches. The variation range of TDS is 26.97~150.20 mg/L, and the average value is 78.74 mg/L. The downstream of the Jinjiang watershed, affected by seawater near the mouth of the sea, has the highest TDS. The cations in Jinjiang watershed are mainly made up of Ca^{2+} and Na^{+}. For Dongxi and Xixi, the Ca^{2+} is the main cation. The Na^{+} in lower reaches is obviously higher than the other two regions. The anions in Jinjiang watershed are mainly made up of HCO_3^- and SO_4^{2-}. For water bodies containing metal minerals such as Fe, Mn, Zn, and Pb, the order from highest to lowest content is Xixi watershed, lower reaches, and Dongxi watershed, respectively. Total nitrogen (TN) and total phosphorus (TP) in the Dongxi watershed are slightly higher than that in the Xixi watershed. The TN and TP are shown in the middle of the others after flowing downstream. The variation coefficients of Ca^{2+} and K^{+} are relatively small, and their contents are mainly controlled by the water-rock action. The variation coefficients of Zn and Pb are greater than 1 (strong variation), showing high volatility and dispersion at different points, which may be influenced by both environmental changes in groundwater and anthropogenic pollution.

Table 1. Descriptive statistics of river water chemical index in Jinjiang watershed (unit: mg/L).

Location	Parameter	pH	TDS	K^+	Na^+	Ca^{2+}	Mg^{2+}	SO_4^{2-}	HCO_3^-	Cl^-	Pb	Fe	Mn	Zn	TN	TP
Dongxi watershed	Min	7.45	26.97	1.69	1.38	1.62	0.21	2.37	11.87	1.04	0.00	0.01	0.00	0.00	0.58	0.03
	Max	9.58	115.80	5.85	11.88	17.77	3.23	13.67	74.20	12.14	0.01	1.29	0.45	0.17	5.87	0.58
	Mean	7.96	78.74	3.82	6.52	10.87	1.67	7.94	41.25	5.85	0.00	0.46	0.13	0.02	2.43	0.19
	SD	0.52	22.96	0.99	2.71	4.04	0.74	2.79	17.08	2.76	0.00	0.34	0.09	0.03	1.21	0.11
	CV/%	6.57	29.16	26.01	41.51	37.19	44.06	35.14	41.42	47.20	160.43	72.95	69.60	188.20	49.79	59.69
Xixi watershed	Min	7.58	47.66	2.35	2.47	4.57	0.49	3.80	0.59	1.73	0.00	0.47	0.06	0.01	0.22	0.02
	Max	8.65	122.60	4.30	19.37	22.17	6.35	51.47	53.42	9.01	0.01	1.44	1.11	0.21	3.59	0.51
	Mean	7.76	78.59	3.02	5.65	11.53	1.84	16.87	25.61	3.97	0.01	0.71	0.26	0.04	1.81	0.24
	SD	0.22	20.12	0.53	3.55	4.00	1.58	12.81	13.95	1.91	0.00	0.21	0.22	0.05	0.91	0.15
	CV/%	2.88	25.60	17.52	62.81	34.67	86.12	75.91	54.46	48.20	75.29	30.23	83.37	116.03	50.15	63.62
Lower reaches	Min	7.48	81.92	4.07	6.68	11.57	1.77	11.56	36.21	6.24	0.00	0.39	0.15	0.01	1.09	0.06
	Max	7.85	150.20	5.82	23.05	17.40	3.84	16.48	59.36	33.63	0.01	1.23	0.35	0.05	3.28	0.50
	Mean	7.61	116.22	4.93	14.72	13.88	2.59	13.35	46.90	19.50	0.00	0.77	0.24	0.03	2.23	0.23
	SD	0.17	36.22	0.81	9.22	2.72	0.96	2.24	9.58	14.40	0.01	0.35	0.09	0.02	0.90	0.19
	CV/%	2.17	31.16	16.49	62.64	19.59	36.91	16.82	20.44	73.85	200.00	45.35	36.93	69.28	40.46	84.99

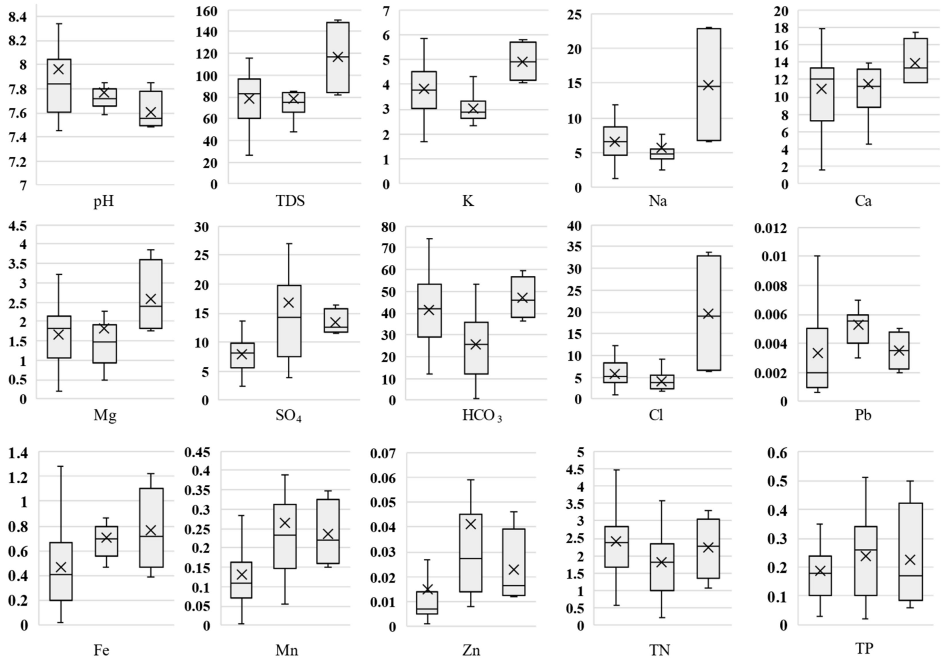

Figure 3. Box plots of river water chemical index in Jinjiang watershed (unit: mg/L). In each plot, the left box represents the Dongxi watershed, the middle box represents the Xixi watershed, and the right box represents the lower reaches.

The Piper trilinear diagram can reflect the composition of ions in water bodies [56]. As shown in Figure 4, the cations are mainly Ca^{2+} and Na^{+}. In the anion triangles, the Dongxi watershed is dominated by HCO_3^{-}, while the composition of the Xixi watershed is mainly made up of SO_4^{2-}. The water chemistry in the Dongxi basin is all HCO_3-Ca type. The water chemistry in the Xixi basin is HCO_3-Ca type with high SO_4^{2-} content in the upper reaches of the basin, and the water chemistry type gradually changes to Cl-Ca type in the lower reaches of Bailai Township. The estuary of Jinjiang watershed, due to the influence of seawater, has a relatively higher proportion of Cl-Na type of water chemistry.

4.2. Evolution of Water Chemical Component Characteristics and Controlling Factors

Hydrochemical components are influenced by both natural factors and human activities. The Gibbs diagram [57] is a way to ensure the dominant natural factors influencing the local hydrochemical components. For study areas, most water samples have a TDS value of around 100 mg/L. So, in Figure S1, the water samples gather in the rock dominance of the Gibbs diagrams. It indicates that hydrochemical components are dominantly governed by rock–water interaction in nature. For the end-member diagram (Figure S2), the samples are located in the silicate-controlling district, which shows that silicate rock weathering has a huge influence [58].

Robust principal component analysis (RPCA) is performed on the CLR-transformed component matrix to obtain component scores and loadings. By using these data, the biplot of compositions analysis and distribution map of the contribution rate of each variable were made (Figures 5 and 6). The first two principal components explain 68.1% of the total variance, with 48.4% by principal component 1 (PC1) and 19.7% by principal component 2 (PC2). The line of SO_4^{2-} is the longest, followed by TP, Ca^{2+}, Mg^{2+}, Na^{+} + K^{+}, TN, Fe, Cl^{-}, and Zn. Among them, Na^{+} + K^{+}, Ca^{2+}, Mg^{2+}, and heavy metal ions, such as Fe, Mn, Zn, and Pb, have a longer projection on the horizontal axis with conventional ions and have a relatively high contribution to PC1. Considering that the upstream of Jinjiang watershed is rich in iron, manganese, zinc, and lead metal mines, and silicate rocks are mainly weathered by the surface water of Jinjiang watershed [59,60], the PC1 is believed to reflect the influence of rock weathering and leaching release from metal minerals mining on the chemical composition of the water. The projections of TN, SO_4^{2-}, and TP on the vertical axis are long and its contribution to PC2 is relatively high. These projections are associated with human activities. Therefore, PC2 mainly explains the influence of agricultural and domestic pollutant discharges on the chemical composition of the water body.

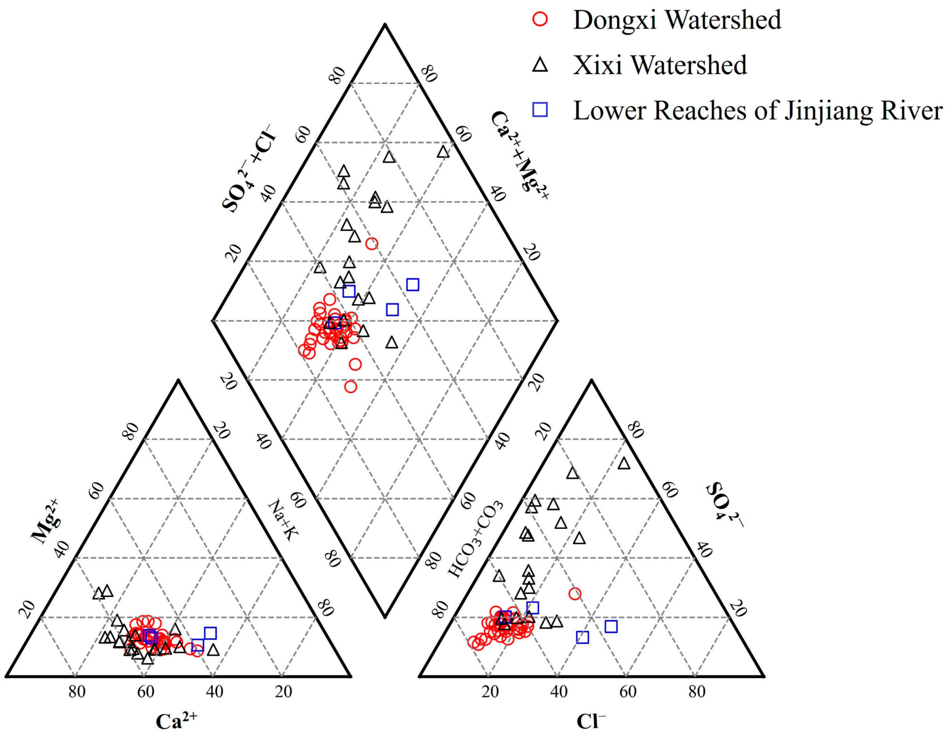

Figure 4. Piper trilinear diagram demonstrating the hydrochemical composition of river water in Jinjiang watershed.

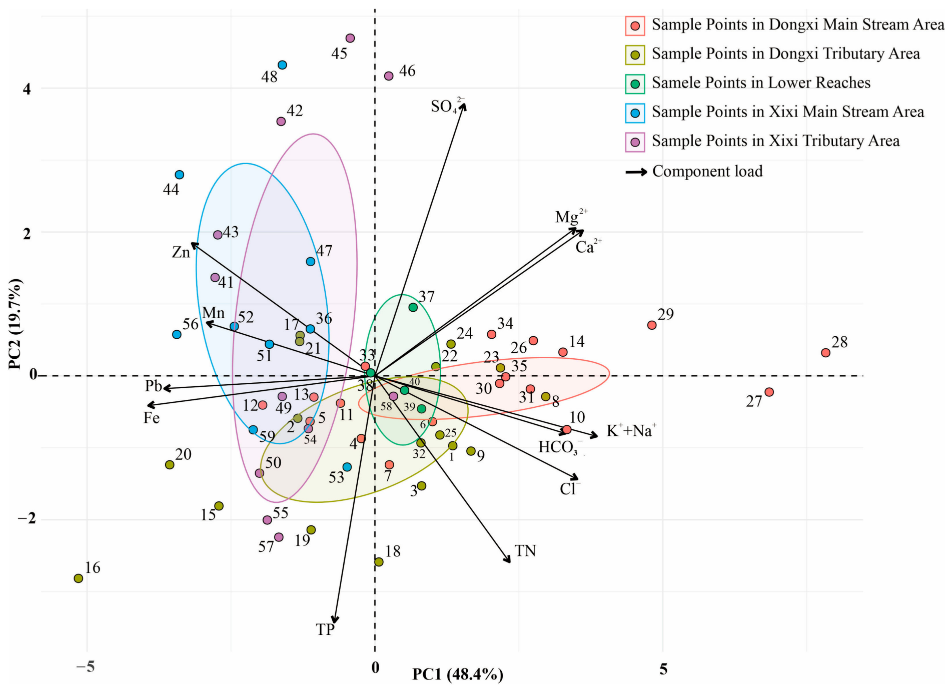

Figure 5. The biplot of all sampled river waters in Jinjiang watershed. The numbers in the figure represent the sample numbers.

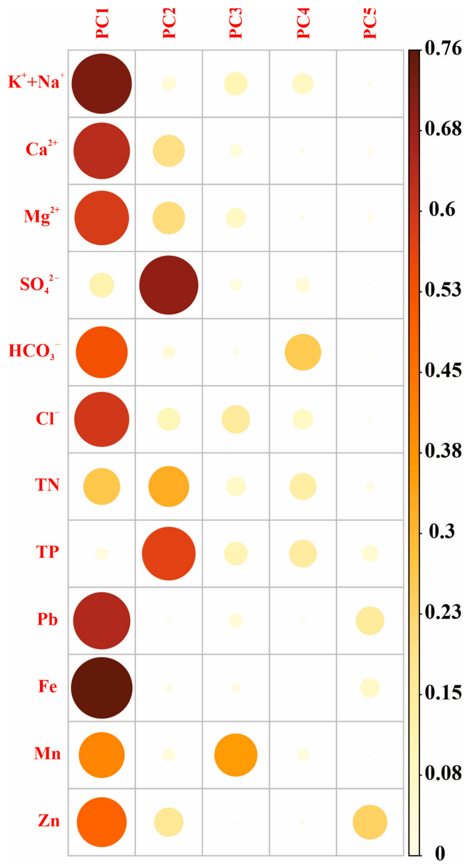

Figure 6. The distribution map of the contribution rate of each hydrochemical index for river water in Jinjiang watershed.

To highlight the trend of data concentration, the samples in different parts are indicated by different colors, and the confidence ellipse with a 99.7% confidence level is constructed by the sample distribution and corresponds to the sampling points by color. The distribution of samples shows that there are obvious differences in the characteristic components in different areas. TP, TN, and Cl^- are characteristic components in the Dongxi watershed, indicating that the chemical composition variation in Dongxi is mainly influenced by the residents and their agricultural production, especially the overdevelopment of the upstream basin of Shanmei reservoir is a direct contributor to nitrogen, phosphorus, and organochlorine pesticides [61,62]. The characteristic components in the Xixi watershed are Fe, Mn, Zn, Pb, etc., which is mainly due to the distribution of minerals containing related elements. A large number of metal mines are distributed from Yidu town in upstream Yongchun County to Jiandou town in the middle reaches of Xixi and the urban area of Anxi County [63], and these mines are the main sources of Fe, Mn, Zn, and Pb in the river. The water samples downstream of Jinjiang watershed are influenced by the complex human activities in the area with the mixed influence of the confluence components of the East and West Creeks. There is a large variability in components, and the main characteristic components are Ca^{2+}, Mg^{2+}, $Na^+ + K^+$, TN, and HCO_3^-.

4.3. Identification of the Water Chemical Composition Change

In Figure 7, the results of the calculation of MD between the basin-wide hydrochemical composition data and the "original composition" are displayed. It reveals that the MD values among the "original composition" samples are quite small, ranging from 2.64 to 3.32. This suggests that the selected original samples exhibit a similar combination of chemical composition. The variation in MD in the Xixi basin ranges from 3.32 to 23.5, indicating relatively minor differences in hydrochemical composition during the rainy season. However, in the Dongxi watershed, except for the samples from the Shanmei reservoir, the MD ranges from 2.64 to 47.4, indicating a significant variation in composition during the rainy season. Prior to the convergence of the East and West Creeks, the MD values between sample 35 of the Dongxi (before its confluence with Xixi) and sample 36 of the Xixi, as well as the "original composition", are all low, which shows little difference in composition. Following the confluence of Dongxi and Xixi, the MD rapidly increased from 3.55 (sample No. 37) to 19.96 (sample No. 39), eventually reaching 86.06 at the estuary. This sharp increase demonstrates a dramatic change in composition, which may be influenced by combined factors of human activities in the downstream city of Quanzhou along Jinjiang and the mixing of seawater where the river meets the sea.

In the Xixi watershed, the Houjing village in Jiandou town, which falls within this sub-basin, is home to a concentration of both coal mines and limestone mines. As the mainstream passes through this area, the mining activities have led to an increase in MD at sampling point 42. Additionally, the concentrations of Ca^{2+}, Mg^{2+}, and SO_4^{2-} in the water composition have also increased. When the tributaries of Shuangxi and Qiyangxi flow into this area, MD at sampling point 44 has consistently remained high. This can be attributed primarily to the presence of numerous sulfur iron ore and coal mines distributed within the watersheds of Shuangxi Creek and Qiyangxi Creek. Additionally, the extensive tea planting in the area contributes to elevated levels of TN, Mn, and Zn in the water. Sampling point 43 represents the composition of Shuangxi Creek and Qiyang Creek. At the confluence of the two tributaries, it is observed that the levels of TN, Mn, and Zn in its composition increase, and its MD continuously fluctuates. The elevated MD at sampling point 50 is attributed to the abnormal increase in TN and TP levels. This phenomenon can be attributed to the sampling site's location in downtown Shangqing town, where it is subject to the impact of domestic sewage from the town. Similarly, sampling point 59 in the downtown city of Nan'an also had an increase in MD due to the increase in the level of TP and TN caused by the influence of domestic sewage.

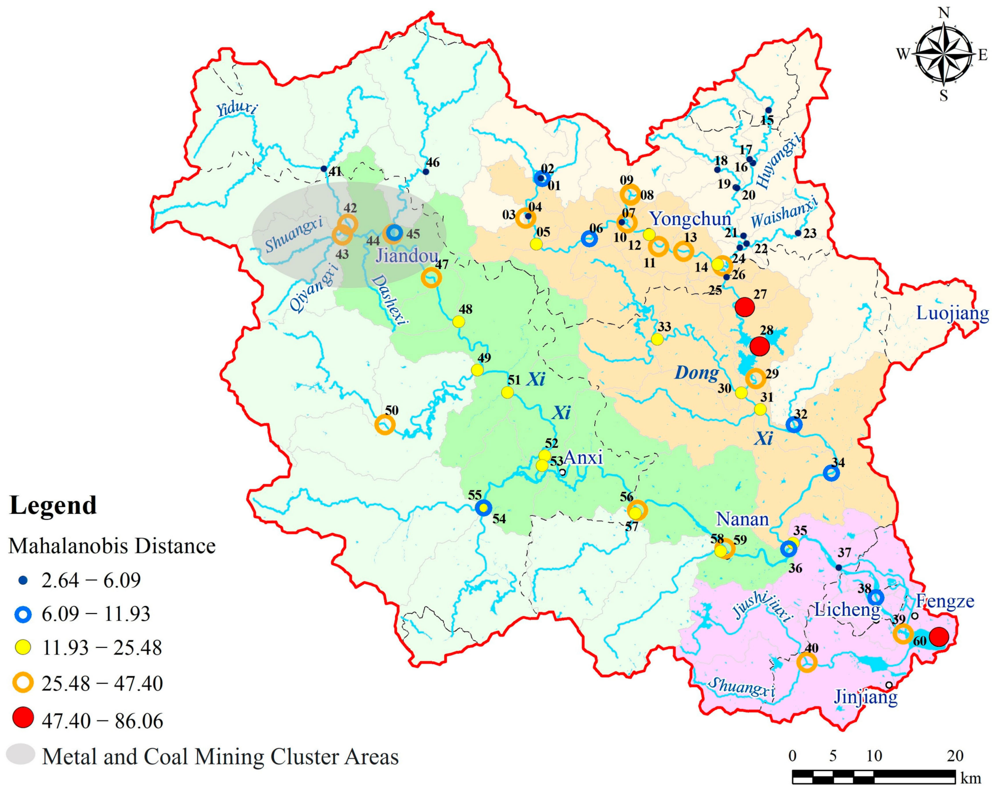

Figure 7. The Mahalanobis distance map of sampled river water in Jinjiang watershed. The numbers in the figure represent the sample numbers.

The same pattern is found in the Dongxi watershed. The elevated MD at sampling point 5 of the mainstream is caused by the confluence of tributaries at sampling point 3, which has different compositions. The elevated MD at sampling point 12 reflects the interference of human activities in Yongchun County with the chemical composition of the river water. The abnormally high values of MD at sampling points 27, 28, and 29 of Shanmei reservoir are mainly due to the large difference between the chemical composition of reservoir water and that of the river water [64]. This proportional difference, an increase when represented in MD, is not due to pollution. Then the decrease in MD at sampling point 31 is because of the recovery of the river's chemical composition. As observed, the MD of the east–west confluence initially exhibits a minor change, but it experiences a significant increase when flowing downstream. This indicates that the human activities and seawater disturbance in the downstream area of Jinjiang watershed results in a substantial alteration in the composition's proportion.

Water samples of the mainstream were added one by one from upstream to downstream, and the centers of components for the mainstreams of Xixi and Dongxi, respectively, were iteratively calculated. The MD from that center at each sampling point was also determined. Using these results, clustered line charts of MD for the mainstem of Dongxi and Xixi were drawn (Figure 7). The mean polyline (black polyline in Figure 8) shows that both Dongxi and Xixi watersheds exhibit a smooth MD for the upstream sample components, indicating that there is less variation among the upstream sample components. The gradual decrease in the middle stream MD shows a trend of gradually decreasing component differences, which indicates that human activities have not yet had a serious impact on the river's chemical composition. In the downstream area of Jinjiang watershed, where human activities are carried out frequently, the MD increases rapidly, reflecting the dramatic changes in the chemical composition caused by the combined disturbance of complex human activities and seawater. The overall covariance structure of the data and the component centers are changing with the continuous addition of samples from the mainstream.

As shown in Figure 8, the clustered line charts of MD in the basin are used to intuitively exhibit the variation in MD along the runoff. In the figure, each polyline is the sample Mahalanobis distance calculated from a single iteration. To highlight the trend produced by the iterations, the color of the polyline in the figure becomes lighter as subsequent sample data are added, where the black polyline is the average of the Mahalanobis distance of the polyline cluster. The horizontal coordinate is the sample number from the upstream to the downstream mainstem.

It can be seen in the clustered line charts of MD in the mainstream of Xixi (Figure 8a) that the variation trend of MD at different places in the mainstream of Xixi shows different or even opposite results. According to the trend of variation of MD, the Xixi is divided from sample point 48 into two areas. The area (I) in the upper reaches mainly represents that the area is little affected by human activities and its chemical composition is close to the "original composition". With the iterative addition of the water chemistry of the mainstream samples, the component centers of the area (I) are gradually moving away from the "original composition". This change results in the different degrees of increase in MD of all samples in the upstream area (I). The area (II) below sample point 48 is greatly affected by human activities. With the iterative addition to the hydrochemical composition of the mainstream samples, the component centers are getting closer to the "non-original composition", resulting in a gradual decrease in MD of the sample composition in the area (II). The rapid increase in component variation in the downstream area of Jinjiang watershed, where the tributaries converge, is reflected in the rapid increase in MD due to the interference of various factors.

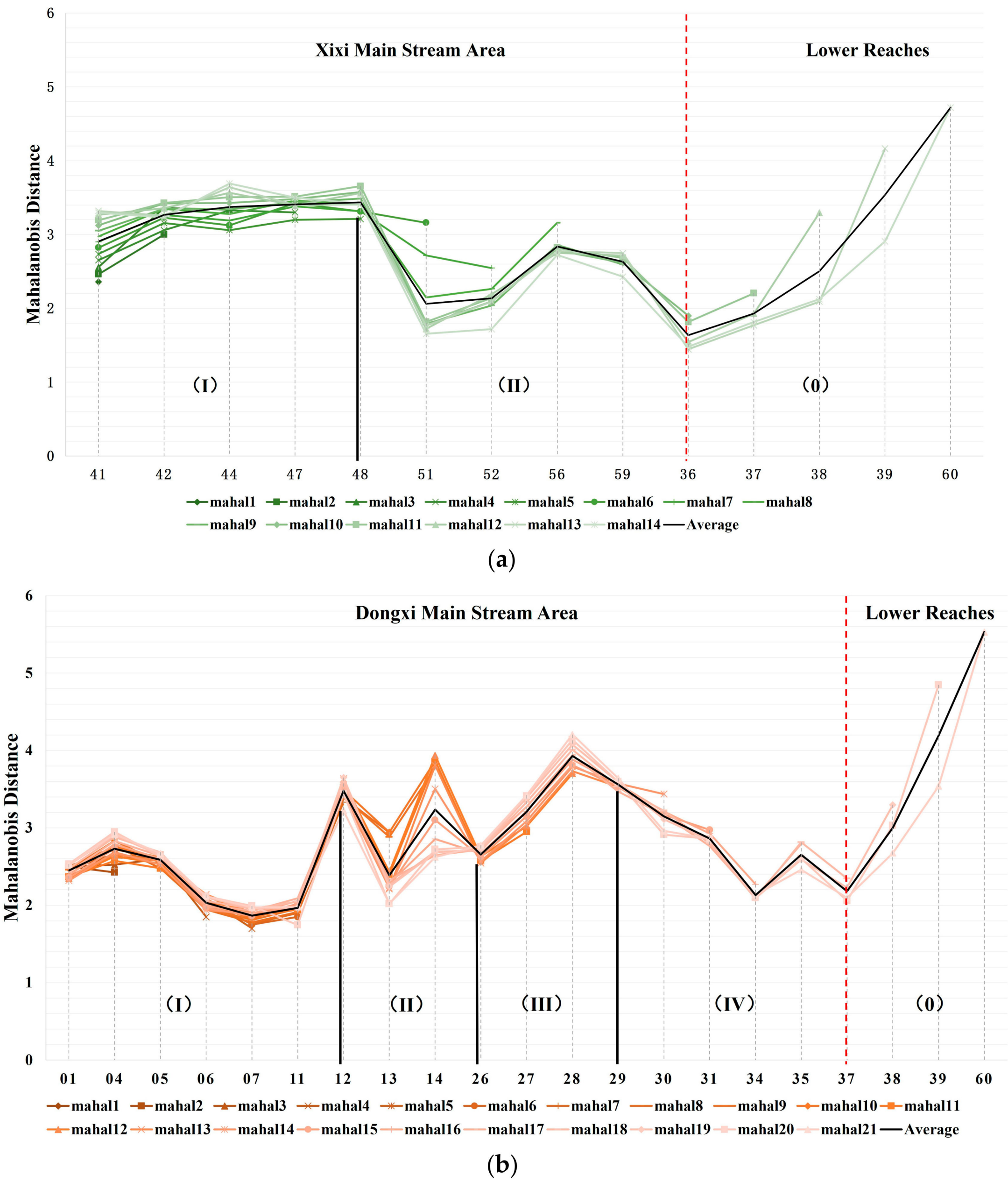

Figure 8. The result of iterative calculation of Mahalanobis distance for the river water of (**a**) Xixi River and (**b**) Dongxi River. Each line represents the Mahalanobis distance of a single iteration calculation. As more sample data is added, the color of the lines in the graph becomes lighter. The black line represents the average Mahalanobis distance of the cluster of lines. The horizontal axis represents the sample number from upstream to downstream. According to different trends, different sub-regions are divided by black vertical lines. The red dashed line represents the boundary between Xixi (Dongxi) and the lower reaches of the main stream and (I), (II), (III), (IV), (0) represent the area numbers of different trends and.

The situation of the mainstream of Dongxi is more complex (Figure 8b), and it can be classified into four distinct areas delineated by sampling points 12, 26, and 28. Area (I) is less disturbed by humans and has a chemical composition that is closer to the "original composition". MD values of samples located in this area will continue to increase with the addition of downstream data, indicating that the river's chemical compositions are constantly being influenced by various integrated factors and therefore move away from the component center. The sampling points 13 and 14 belong to the area (II) and are located within Yongchun County. With the addition of the data, the MD of sample 13 is showing a downward trend, while the MD of sample 14 is increasing. This is mainly because the urban area of Yongchun County is the most densely populated region in the northern mountainous area, and the component changes are generated by the inflow of industrial and domestic pollutants. MD of area (III) is at a high level, which reflects the large difference in chemical composition among the reservoir, lake water, and river water.

The (0) region in Figure 8a,b shows the variational tendency of Mahalanobis distance in lower reaches. It can be seen in both figures that the overall trend of Mahalanobis distance in the region (0) increases sharply, and the single-point Mahalanobis distance decreases with the addition of downstream data. Due to the fact of more interference from human activities, there are sharp differences between the compositions of each water sample, resulting in a sharp increase in Mahalanobis distance. At the same time, since the addition of various downstream data, the composition center deviates from the "original composition" to the downstream composition, so it also shows a decrease in the Mahalanobis distance for a single point in the lower reaches.

5. Conclusions

The compositional data analysis method (CoDA) was proposed from the perspective of compositional data analysis theory, considering the geochemical riverine system as a whole to detect changes in the composition of the entire watershed. A total of 60 water samples were collected and analyzed using traditional analytical methods. Based on this, further analysis of the transformed water chemistry composition data was carried out using RPCA, biplot, and Mahalanobis distance, leading to the following conclusions:

(1) The characteristic components of water bodies in Jinjiang watershed show obvious variability and complex evolutionary characteristics from upstream to downstream. Influenced by the weathering of silicate rocks, the water chemical composition of Jinjiang is mainly composed of Ca^{2+} and Na^{+} cations. The anion of East River is mainly made up of HCO_3^-, and the water chemistry is of HCO_3-Ca type. The anions of the West Stream are dominated by SO_4^{2-}, and the water chemistry of the upper and middle streams is of HCO_3-Ca type with high SO_4^{2-}. The water chemistry type gradually changes to Cl-Ca type in the lower reaches of Bailai Township. The estuary of Jinjiang, due to the influence of seawater, has a relatively higher proportion of Cl-Na type of water chemistry.

(2) The CoDA method served as a valuable tool for identifying and explaining anomalies in the hydrochemistry components within the basin. By comparing the MD value with the central "original component" of Jinjiang, it accurately identifies areas in the basin with outlier water chemistry compositions. The results obtained from RPCA analysis reveal that rock weathering, mining, and agricultural pollution are the primary factors that influence the hydrochemistry components. It is remarkable that the elements such as Fe, Mn, Zn, and Pb originating from mining activities become the distinctive components in the Xixi River basin. The Dongxi River, on the other hand, exhibits characteristic components including TP, TN, and Cl^-, indicating the influence of domestic and agricultural pollution.

This paper reveals the spatial variability in surface water in hydrochemical terms in Jinjiang watershed and discusses its underlying controlling factors. The findings can be utilized as a reference for investigating the hydrochemical spatial differences in other river basins.

Supplementary Materials: The following supporting information can be downloaded at: https://www.mdpi.com/article/10.3390/w16010045/s1, Figure S1: Gibbs Map of all samples in Jinjiang River Basin, Figure S2: End-member diagram of all samples in Jinjiang River Basin.

Author Contributions: Y.Z. (Yuchen Zhu): Field investigation, data curation, formal analysis, and writing—original draft. H.Y.: Formal analysis and writing—original draft and editing. Y.X.: Conceptualization and writing—review and editing. Q.H.: Conceptualization and writing—review and editing. Y.L.: Conceptualization, funding acquisition, and supervision. J.L.: Methodology and formal analysis. L.W.: Field investigation and data curation. Y.Z. (Yuqing Zhang): Field investigation, data curation and methodology. W.H.: Field investigation, data curation, and formal analysis. J.W.: Field investigation and data curation. All authors have read and agreed to the published version of the manuscript.

Funding: This research was funded by [Fujian Provincial Key Laboratory of Water Cycling and Eco-Geological Processes] grant number [SK202305KF01], [the China Geological Survey's project] grant number [DD20190303, DD20230459], [the Natural Science Foundation of China] grant number [42007183], [the Natural Science Foundation of Sichuan Province] grant number [2022NSFSC1084], [the Student Research Training Program of Southwest Jiaotong University] grant number [202310613077], [the Fundamental Research Funds for the Central Universities] grant number [2682022ZTPY002, 2682022ZTPY088].

Data Availability Statement: The data presented in this study are available on request from the first author.

Conflicts of Interest: The authors declare that they have no known competing financial interests or personal relationships that could have appeared to influence the work reported in this paper.

References

1. Yang, H.J.; Xiao, Y.; Hao, Q.C.; Wang, L.W.; Zhang, Y.Q.; Liu, K.; Zhu, Y.C.; Liu, G.X.; Yin, S.Y.; Xie, Z. Geochemical characteristics, mechanisms and suitability for sustainable municipal and agricultural water supply of confined groundwater in central North China Plain. *Urban Clim.* **2023**, *49*, 101459. [CrossRef]
2. Shi, W.; Xia, J.; Gippel, C.J.; Chen, J.X.; Hong, S. Influence of disaster risk, exposure and water quality on vulnerability of surface water resources under a changing climate in the Haihe River basin. *Water Int.* **2017**, *42*, 462–485. [CrossRef]
3. Yuan, Z.; Yan, D.H.; Yang, Z.Y.; Yin, J.; Zhang, C.; Yuan, Y. Projection of surface water resources in the context of climate change in typical regions of China. *Hydrol. Sci. J.* **2017**, *62*, 283–293. [CrossRef]
4. Xiao, Y.; Hao, Q.C.; Zhang, Y.H.; Zhu, Y.C.; Yin, S.Y.; Qin, L.M.; Li, X.H. Investigating sources, driving forces and potential health risks of nitrate and fluoride in groundwater of a typical alluvial fan plain. *Sci. Total Environ.* **2022**, *802*, 149909. [CrossRef]
5. Ewuzie, U.; Nnorom, I.C.; Ugbogu, O.C.; Onwuka, C.V. Hydrogeochemical, microbial and compositional analysis of data from surface and groundwater sources in Southeastern Nigeria. *J. Geochem. Explor.* **2021**, *224*, 106737. [CrossRef]
6. Wang, H.; Sun, L.; Du, P. Surface Water Quality Assessment in Main Stream of Liaohe River. *Adv. Mater. Res.* **2013**, *788*, 354–358. [CrossRef]
7. Gao, F.; Feng, G.; Han, M.; Dash, P.; Jenkins, J.; Liu, C. Assessment of Surface Water Resources in the Big Sunflower River Watershed Using Coupled SWAT–MODFLOW Model. *Water* **2019**, *11*, 528. [CrossRef]
8. Xiao, Y.; Liu, K.; Hao, Q.C.; Li, Y.S.; Xiao, D.; Zhang, Y.J. Occurrence, Controlling Factors and Health Hazards of Fluoride-Enriched Groundwater in the Lower Flood Plain of Yellow River, Northern China. *Expo. Health* **2022**, *14*, 345–358. [CrossRef]
9. Xiao, Y.; Liu, K.; Hao, Q.C.; Xiao, D.; Zhu, Y.C.; Yin, S.Y.; Zhang, Y.H. Hydrogeochemical insights into the signatures, genesis and sustainable perspective of nitrate enriched groundwater in the piedmont of Hutuo watershed, China. *CATENA* **2022**, *212*, 106020. [CrossRef]
10. Buccianti, A. The FOREGS repository: Modelling variability in stream water on a continental scale revising classical diagrams from CoDA (compositional data analysis) perspective. *J. Geochem. Explor.* **2015**, *154*, 94–104. [CrossRef]
11. Guggenmos, M.R.; Daughney, C.J.; Jackson, B.M.; Morgenstern, U. Regional-scale identification of groundwater-surface water interaction using hydrochemistry and multivariate statistical methods, Wairarapa Valley, New Zealand. *Hydrol. Earth Syst.* **2011**, *15*, 3383–3398. [CrossRef]
12. Zhang, B.; Song, X.F.; Zhang, Y.H.; Ma, Y.; Tang, C.Y.; Yang, L.H.; Wang, Z.L. The interaction between surface water and groundwater and its effect on water quality in the Second Songhua River basin, northeast China. *J. Earth Syst. Sci.* **2016**, *125*, 1495–1507. [CrossRef]
13. Zhao, W.; Lin, Y.Z.; Zhou, P.P.; Wang, G.C.; Dang, X.Y.; Gu, X.F. Characteristics of groundwater in Northeast Qinghai-Tibet Plateau and its response to climate change and human activities: A case study of Delingha, Qaidam Basin. *China Geol.* **2021**, *4*, 377–388. [CrossRef]
14. Dall'Agnol, R.; Sahoo, P.K.; Salomão, G.N.; de Araújo, A.D.M.; da Silva, M.S.; Powell, M.A.; Junior, J.F.; Ramos, S.J.; Martins, G.C.; da Costa, M.F.; et al. Soil-sediment linkage and trace element contamination in forested/deforested areas of the Itacaiúnas River Watershed, Brazil: To what extent land-use change plays a role? *Sci. Total Environ.* **2022**, *828*, 154327. [CrossRef] [PubMed]
15. Ma, H.Y.; Zhu, G.F.; Zhang, Y.; Pan, H.X.; Guo, H.W.; Jia, W.X.; Zhou, J.J.; Yong, L.L.; Wan, Q.Z. The effects of runoff on Hydrochemistry in the Qilian Mountains: A case study of Xiying River Basin. *Environ. Earth Sci.* **2019**, *78*, 385. [CrossRef]
16. Goonetilleke, A.; Vithanage, M. Water Resources Management: Innovation and Challenges in a Changing World. *Water* **2017**, *9*, 281. [CrossRef]
17. Zhai, R.; Tao, F.L.; Chen, Y.; Dai, H.C.; Liu, Z.W.; Fu, B.J. Future water security in the major basins of China under the 1.5 °C and 2.0 °C global warming scenarios. *Sci. Total Environ.* **2022**, *849*, 157928. [CrossRef]

18. Yang, L.; Zhao, G.J.; Tian, P.; Mu, X.M.; Tian, X.J.; Feng, J.H.; Bai, Y.P. Runoff changes in the major river basins of China and their responses to potential driving forces. *J. Hydrol.* **2022**, *607*, 127536. [CrossRef]
19. Hao, Q.C.; Li, Y.S.; Xiao, Y.; Yang, H.J.; Zhang, Y.Q.; Wang, L.W.; Liu, K.; Liu, G.X.; Wang, J.; Hu, W.X.; et al. Hydrogeochemical fingerprint, driving forces and spatial availability of groundwater in a coastal plain, Southeast China. *Urban Clim.* **2023**, *51*, 101611. [CrossRef]
20. Vareda, J.; Valente, A.; Durães, L. Assessment of heavy metal pollution from anthropogenic activities and remediation strategies: A review. *J. Environ. Manag.* **2019**, *246*, 101–118. [CrossRef]
21. Yang, Z.; Zhou, Y.X.; Wenninger, J.; Uhlenbrook, S.; Wang, X.S.; Wan, L. Groundwater and surface-water interactions and impacts of human activities in the Hailiutu catchment, northwest China. *Hydrogeol. J.* **2017**, *25*, 1341–1355. [CrossRef]
22. Kumar, V.; Parihar, R.; Sharma, A.; Bakshi, P.; Sidhu, G.P.S.; Bali, A.; Karaouzas, I.; Bhardwaj, R.; Thukral, A.; Gyasi-Agyei, Y.; et al. Global evaluation of heavy metal content in surface water bodies: A meta-analysis using heavy metal pollution indices and multivariate statistical analyses. *Chemosphere* **2019**, *236*, 124364. [CrossRef] [PubMed]
23. Gad, M.; Elsayed, S.; Moghanm, F.S.; Almarshadi, M.H.; Alshammari, A.S.; Khedher, K.M.; Eid, E.M.; Hussein, H. Combining Water Quality Indices and Multivariate Modeling to Assess Surface Water Quality in the Northern Nile Delta, Egypt. *Water* **2020**, *12*, 2142. [CrossRef]
24. Zheng, L.L.; Jiang, C.L.; Chen, X.; Li, Y.H.; Li, C.; Zheng, L.G. Combining hydrochemistry and hydrogen and oxygen stable isotopes to reveal the influence of human activities on surface water quality in Chaohu Lake Basin. *J. Environ. Manag.* **2022**, *312*, 114933. [CrossRef] [PubMed]
25. Benadela, L.; Bekkoussa, B.; Gaidi, L. Multivariate analysis and geochemical investigations of groundwater in a semi-arid region, case of superficial aquifer in Ghriss Basin, Northwest Algeria. *J. Groundw. Sci. Eng.* **2022**, *10*, 233–249.
26. Ismail, A.H.; Shareef, M.A.; Mahmood, W. Hydrochemical characterization of groundwater in Balad district, Salah Al-Din Governorate, Iraq. *J. Groundw. Sci. Eng.* **2018**, *6*, 306–322. [CrossRef]
27. Blake, S.; Henry, T.; Murray, J.; Flood, R.H.; Muller, M.R.; Jones, A.G.; Rath, V.J.A.G. Compositional multivariate statistical analysis of thermal groundwater provenance: A hydrogeochemical case study from Ireland. *Appl. Geochem.* **2016**, *75*, 171–188. [CrossRef]
28. Bahrami, M.; Khaksar, E.; Khaksar, E. Spatial variation assessment of groundwater quality using multivariate statistical analysis(Case Study: Fasa Plain, Iran). *J. Groundw. Sci. Eng.* **2020**, *8*, 230–243. [CrossRef]
29. Flem, B.E.; Reimann, C.; Fabian, K.; Birke, M.; Filzmoser, P.; Banks, D. Graphical statistics to explore the natural and anthropogenic processes influencing the inorganic quality of drinking water, ground water and surface water. *Appl. Geochem.* **2017**, *88*, 133–148. [CrossRef]
30. Gozzi, C.; Filzmoser, P.; Buccianti, A.; Vaselli, O.; Nisi, B. Statistical methods for the geochemical characterisation of surface waters: The case study of the Tiber River basin (Central Italy). *Comput. Geosci.* **2019**, *131*, 80–88. [CrossRef]
31. Ahmed, M.T.; Monir, M.U.; Hasan, M.Y.; Rahman, M.M.; Rifat, M.S.I.; Islam, M.N.; Khan, A.S.; Rahman, M.M.; Islam, M.S. Hydro-geochemical evaluation of groundwater with studies on water quality index and suitability for drinking in Sagardari, Jashore. *J. Groundw. Sci. Eng.* **2020**, *8*, 259–273.
32. Wu, H.F.; Chen, Y.; Chen, X.W.; Liu, M.B.; Gao, L.; Deng, H.J. A new approach for optimizing rain gauge networks: A case study in the Jinjiang Basin. *Water* **2020**, *12*, 2252. [CrossRef]
33. Meng, H.B.; Zhang, J.; Zheng, Z. Retrieving Inland Reservoir Water Quality Parameters Using Landsat 8-9 OLI and Sentinel-2 MSI Sensors with Empirical Multivariate Regression. *Int. J. Environ. Res. Public Health* **2022**, *19*, 7725. [CrossRef] [PubMed]
34. Lin, F.; Chen, X.W.; Yao, H.X.; Lin, F.Y. SWAT model-based quantification of the impact of land-use change on forest-regulated water flow. *CATENA* **2022**, *211*, 105975. [CrossRef]
35. Liu, Y.C.; Wu, L.; Shi, G.W.; Cao, S.W.; Li, Y.S. Characteristics and sources of microplastic pollution in the water and sediments of the Jinjiang River Basin, Fujian Province, China. *China Geol.* **2022**, *5*, 429–438. [CrossRef]
36. Liu, X.Y.; Wei, M.; Zeng, J. Simulating urban growth scenarios based on ecological security pattern: A case study in Quanzhou, China. *Int. J. Environ. Res. Public Health* **2020**, *17*, 7282. [CrossRef]
37. Li, C.J.; Pan, C.Z.; Teng, Y.G. Rainfall-runoff and pollution characteristics of tea garden in Xixi watershed within Jinjiang River basin. *Chin. J. Environ. Eng.* **2013**, *7*, 2909–2914.
38. Lu, Y.M.; Zhang, H.; Shao, W. Prediction of river water quality considering spatiotemporal correlation and meteorological factors. In Proceedings of the 2021 9th International Conference on Agro-Geoinformatics (Agro-Geoinformatics), Shenzhen, China, 26–29 July 2021; pp. 1–5.
39. Wu, J.H.; Wang, Z.C. A hybrid model for water quality prediction based on an artificial neural network, wavelet transform, and long short-term memory. *Water* **2022**, *14*, 610. [CrossRef]
40. Li, Y.S.; Liu, C.L.; Hao, Q.C. *Report on Comprehensive Geological Survey of Xiamen-Zhangzhou-Quanzhou City*; Chinese Academy of Geological Sciences, The Institute of Hydrogeology and Environmental Geology: Shijiazhuang, China, 2021.
41. Nong, X.Z.; Shao, D.G.; Zhong, H.; Liang, J.K. Evaluation of water quality in the South-to-North Water Diversion Project of China using the water quality index (WQI) method. *Water Res.* **2020**, *178*, 115781. [CrossRef]
42. Wu, Y.H.; Zhou, N.Q.; Wu, Z.J.; Lu, S.S.; Cai, Y. Carbon, nitrogen and phosphorus coupling relationships and their influencing factors in the critical zone of Dongting Lake wetlands, China. *J. Groundw. Sci. Eng. Geol.* **2022**, *10*, 250–266.
43. Zhou, Y.H.; Li, P.Y.; Chen, M.J.; Dong, Z.H.; Lu, C.Y. Groundwater quality for potable and irrigation uses and associated health risk in southern part of Gu'an County, North China Plain. *Environ. Geochem. Health* **2021**, *43*, 813–835. [CrossRef] [PubMed]

44. Rollinson, H.R.; Rollinson, H.; Pease, V. *Using Geochemical Data: To Understand Geological Processes*; Cambridge University Press: Cambridge, UK, 2021.
45. Pawlowsky-Glahn, V.; Egozcue, J.J.; Tolosana-Delgado, R. *Modeling and Analysis of Compositional Data*; John Wiley & Sons: Hoboken, NJ, USA, 2015.
46. Aitchison, J. The statistical analysis of compositional data. *J. R. Stat. Soc. Ser. B Methodol.* **1982**, *44*, 139–160. [CrossRef]
47. Buccianti, A.; Mateu-Figueras, G.; Pawlowsky-Glahn, V. *Compositional Data Analysis in the Geosciences: From Theory to Practice*; Geological Society of London: London, UK, 2006.
48. Gabriel, K.R. The biplot graphic display of matrices with application to principal component analysis. *Biometrika* **1971**, *58*, 453–467. [CrossRef]
49. Greenacre, M.; Aitchison, J. Biplots of compositional data. *Appl. Stat.* **2002**, *51*, 375–392.
50. Daunis-i-Estadella, J.; Barceló-Vidal, C.; Buccianti, A. Exploratory compositional data analysis. *Geol. Soc. Lond. Spec. Publ.* **2006**, *264*, 161–174. [CrossRef]
51. De Maesschalck, R.; Jouan-Rimbaud, D.; Massart, D.L. The Mahalanobis Distance. Chemometrics and Intelligent Laboratory Systems. *Am. J. Ind. Bus. Manag.* **2000**, *50*, 1–18.
52. Filzmoser, P.; Ruiz-Gazen, A.; Thomas-Agnan, C. Identification of local multivariate outliers. *Stat. Pap.* **2014**, *55*, 29–47. [CrossRef]
53. Ghorbani, H. Mahalanobis distance and its application for detecting multivariate outliers. *Facta Univ. Ser. Math. Inform.* **2019**, 583–595. [CrossRef]
54. Jouan-Rimbaud, D.; Massart, D.; Saby, C.; Puel, C. Characterisation of the representativity of selected sets of samples in multivariate calibration and pattern recognition. *Anal. Chim. Acta* **1997**, *350*, 149–161. [CrossRef]
55. Templ, M.; Hron, K.; Filzmoser, P. robCompositions: An R-package for robust statistical analysis of compositional data. *Compos. Data Anal. Theory Appl.* **2011**, 341–355.
56. Yang, H.J.; Xiao, Y.; Zhang, Y.Q.; Wang, L.W.; Wang, J.; Hu, W.X.; Liu, G.X.; Liu, F.; Hao, Q.C.; Wang, C. Lithology controls on the mixing behavior and discharge regime of thermal groundwater in the Bogexi geothermal field on Tibetan Plateau. *J. Hydrol.* **2023**, *628*, 130523. [CrossRef]
57. Gibbs, R.J. Mechanisms Controlling World Water Chemistry. *Science* **1970**, *170*, 1088–1090. [CrossRef] [PubMed]
58. Gaillardet, J.; Dupré, B.; Louvat, P.; Allegre, C. Global silicate weathering and CO_2 consumption rates deduced from the chemistry of large rivers. *Chem. Geol.* **1999**, *159*, 3–30. [CrossRef]
59. Yu, R.L.; Hu, G.R.; Lin, C.Q.; Yang, Q.L.; Zhang, C.C.; Wang, X.M. Contamination of heavy metals and isotopic tracing of Pb in intertidal surface sediments of Jinjiang River Estuary, SE China. *Appl. Geochem.* **2017**, *83*, 41–49. [CrossRef]
60. Chen, H.Y.; Teng, Y.G.; Wang, J.S.; Song, L.T. Source apportionment of water pollution in the Jinjiang River (China) using factor analysis with nonnegative constraints and support vector machines. *Environ. Forensics* **2012**, *13*, 175–184. [CrossRef]
61. Yang, D.; Qi, S.H.; Zhang, J.Q.; Wu, C.X.; Xing, X.L. Organochlorine pesticides in soil, water and sediment along the Jinjiang River mainstream to Quanzhou Bay, southeast China. *Ecotoxicol. Environ. Saf.* **2013**, *89*, 59–65. [CrossRef]
62. de Azeredo Morgado, M.G.; Passos, C.J.S.; Garnier, J.; de Lima, L.A.; de Alcântara Mendes, R.; Samson-Brais, É.; Lucotte, M. Large-scale agriculture and environmental pollution of ground and surface water and sediment by pesticides in the Brazilian Amazon: The case of the Santarém region. *Water Air Soil Pollut.* **2023**, *234*, 150. [CrossRef]
63. The People's Government of Quanzhou City. *The Overall Plan of Mineral Resources(2016–2020)*; The People's Government of Quanzhou City: Quanzhou, China, 2017.
64. Yu, N.X.; Qin, Y.; Hao, F.; Lang, Y.C.; Wang, F.S. Using seismic surveys to investigate sediment distribution and to estimate burial fluxes of OC, N, and P in a canyon reservoir. *Acta Geochim.* **2019**, *38*, 785–795. [CrossRef]